

Coupling between phonons and intrinsic Josephson oscillations in cuprate superconductors

F. Forsthofer, Ch. Helm, Ch. Preis, and J. Keller,
 Institut für Theoretische Physik, Universität Regensburg, D-93040 Regensburg, Germany
 K. Schlenga, R. Kleiner, and P. Müller,
 Physikalisches Institut III, Universität Erlangen-Nürnberg, D-91058 Erlangen, Germany
 (December 2, 2024)

The recently reported subgap structures observed in the current-voltage characteristic of intrinsic Josephson junctions in the high- T_c superconductors $Tl_2Ba_2Ca_2Cu_3O_{10+\delta}$ and $Bi_2Sr_2CaCu_2O_{8+\delta}$ are explained by the coupling between c-axis phonons and Josephson oscillations. A model is developed where c-axis lattice vibrations between adjacent superconducting multilayers are excited by the Josephson oscillations in a resistive junction. The voltages of the lowest structures correspond well to the frequencies of longitudinal c-axis phonons with large oscillator strength in the two materials, providing a new measurement technique for this quantity.

The transport properties of highly anisotropic cuprate superconductors in c-direction can well be described by a stack of Josephson junctions formed by non-superconducting material between adjacent superconducting copper oxide multi-layers [1]. Recently the observation of subgap structures in the current-voltage (I - V)-characteristic of intrinsic Josephson junctions in the high- T_c superconductors $Tl_2Ba_2Ca_2Cu_3O_{10+\delta}$ (TBCCO) and $Bi_2Sr_2CaCu_2O_{8+\delta}$ (BSCCO) has been reported [2,3]. Each individual branch of the I - V -curve shows a structure which can be traced back to the I - V -characteristic of one single Josephson junction in the resistive state. These structures seem to be an intrinsic effect, as they have been observed both in step edge junctions (TBCCO) and mesa-type stacks (BSCCO) of different sizes. The characteristic voltages are completely independent of temperature and external magnetic fields, which rules out any relation to the superconducting gap, vortex flow or the thermal excitation of quasiparticles.

It was shown that the pattern of one junction can be described phenomenologically by a resistively shunted junction (RSJ) model by assuming ad hoc a special structure for the current-voltage characteristic of the quasiparticles [3]. It was argued that such a structure might result from peaks in the quasiparticle density of states due to Andreev reflection between normal and superconducting regions. Several alternative approaches, including the modulation of the tunneling distance due to Raman-active phonons, have been mentioned in [2], but up to now all suggestions failed to explain the main features of the effect. In this paper we want to discuss a different mechanism involving phonons by assuming that the local electric field oscillations produced by the Josephson effect in a single junction excite infrared active c-axis phonons. In the following we will present a simple model where we couple the non-linear current-phase relation of one junction to a local oscillator. The analytical and numerical solution of this model provides a very good quantitative explanation of the experimental data. It is shown that the peaks in the subgap structure of the dc

current-voltage characteristic correspond to zeros of the dielectric function of the junction material, i.e. to longitudinal optical phonons.

In the RSJ model the total current (density)

$$i = j_c \sin \gamma + \sigma_0 E + \dot{D}, \quad (1)$$

through one of the junctions is the sum of the Josephson current, the (ohmic) quasiparticle current $I_{qp} = \sigma_0 E$ and the displacement current density \dot{D} , where the (gauge invariant) phase difference γ is related to the electric field E in the barrier of thickness b by

$$\hbar \dot{\gamma} = 2eEb. \quad (2)$$

The displacement current \dot{D} contains the polarization P of the barrier medium, $D = \epsilon_0 E + P = \epsilon_0 \epsilon E$. In the case of high frequency Josephson oscillations in the range of phonon frequencies it is important to keep the full frequency dependence of $\epsilon(\omega)$ or to treat the polarization P as an additional dynamical variable.

Here we assume that the polarization $P = nqz$ is due to a c-axis displacement z of ions with charge q , mass M and density n in the insulating barrier between the copper oxide (multi)-layers. For the motion of the ions we assume a simple oscillator

$$\ddot{z} + \omega_0^2 z + r\dot{z} = \frac{q}{M} E, \quad (3)$$

which is driven by the electric field E in the barrier. In this model the contribution of the oscillator to the dielectric function is given by

$$\epsilon_{ph}(\omega) = 1 + \frac{nq^2}{\epsilon_0 M} \frac{1}{\omega_0^2 - \omega^2 + ir\omega}. \quad (4)$$

It is useful to introduce normalized quantities: First Eq. (1) and (3) are divided by the critical current density j_c , then a characteristic time variable $\tau = t\omega_c$ with $\omega_c = (2e/\hbar)V_c$ is introduced, where $V_c = RI_c = bj_c/\sigma_0$ is the

characteristic voltage determined experimentally by the voltage on the resistive branch at the critical current. Then we obtain

$$j = \sin \gamma + \dot{\gamma} + \beta_c \ddot{\gamma} + \dot{p}, \quad (5)$$

$$\lambda \dot{\gamma} = \ddot{p} + \Omega^2 p + \rho \dot{p}, \quad (6)$$

with the normalized polarization $p = P\omega_c/j_c$, frequency $\Omega = \omega_0/\omega_c$, friction $\rho = r/\omega_c$ and the McCumber parameter $\beta_c = RC\omega_c = \omega_c^2/\omega_J^2$, where $\omega_J^2 = 2ebj_c/(\hbar\epsilon_0)$ is the square of the Josephson plasma frequency and $C = \epsilon_0 F/b$ is the capacitance of the barrier. The coupling constant $\lambda = \omega_{\text{ion}}^2/\omega_J^2 = S(\omega_0^2/\omega_J^2)$ can be expressed by the ionic plasma frequency $\omega_{\text{ion}}^2 = nq^2/(M\epsilon_0)$ or the oscillator strength S of the lattice vibration. In the present case the ratio between the phonon frequency ω_0 and the Josephson plasma frequency ω_J is large; therefore even a small oscillator strength $S = (\omega_{\text{ion}}^2/\omega_0^2)$ can lead to a sizable coupling.

The equations (5) and (6) for the phase and the lattice displacement can be solved numerically to yield $\gamma(t)$ as a function of the current density j through the junction. Taking a time average of the phase the dc current-voltage characteristic is obtained.

As we know from the numerical results (cf. fig. 2 and 3 below) that both the phase and polarization oscillate primarily with one frequency we make the following ansatz

$$\gamma = \gamma_0 + vt + \gamma_1 \sin \omega t, \quad (7)$$

$$p = p_0 + p_1 \cos(\omega t + \varphi). \quad (8)$$

Here v is the time averaged phase velocity, which corresponds to the dc voltage $v = \langle V \rangle / V_c$ in the resistive state.

The different Fourier components of the equations of motion are obtained by the Bessel function expansion

$$\sin \gamma(t) = \sum_{n=-\infty}^{\infty} J_n(\gamma_1) \sin(\gamma_0 + vt + n\omega t). \quad (9)$$

The Josephson current contributes to the dc current only if $v + n\omega = 0$.

For the fundamental harmonic we obtain $\omega = v$. Using this ansatz in the differential equations (5) and (6) we obtain a set of equations for the amplitudes of the different Fourier components. For the constant terms and the coefficients of $\sin vt$ and $\cos vt$ we find:

$$j = -J_1(\gamma_1) \sin \gamma_0 + v, \quad (10)$$

$$\lambda v = \Omega^2 p_0 \quad (11)$$

$$0 = (J_0(\gamma_1) - J_2(\gamma_1)) \cos \gamma_0 - v^2 \beta \gamma_1 - v p_1 \cos \varphi, \quad (12)$$

$$0 = (v^2 - \Omega^2) p_1 \sin \varphi - v \rho p_1 \cos \varphi \quad (13)$$

$$0 = (J_0(\gamma_1) + J_2(\gamma_1)) \sin \gamma_0 + v \gamma_1 - v p_1 \sin \varphi, \quad (14)$$

$$\lambda v \gamma_1 = -(v^2 - \Omega^2) p_1 \cos \varphi - v \rho p_1 \sin \varphi. \quad (15)$$

We can eliminate the polarization and get an equation of motion for the phase oscillation alone:

$$j = v(1 + \frac{1}{2}\sigma(v)\gamma_1^2), \quad (16)$$

$$(J_0(\gamma_1) - J_2(\gamma_1)) \cos \gamma_0 = v^2 \beta_{\text{eff}}(v) \gamma_1, \quad (17)$$

$$J_1(\gamma_1) \sin \gamma_0 = -\frac{1}{2}v\sigma(v)\gamma_1^2 \quad (18)$$

with

$$\beta_{\text{eff}}(v) = \beta - \frac{\lambda(v^2 - \Omega^2)}{(v^2 - \Omega^2)^2 + v^2 \rho^2}, \quad (19)$$

$$\sigma(v) = 1 + \frac{\lambda v^2 \rho}{(v^2 - \Omega^2)^2 + v^2 \rho^2}. \quad (20)$$

The functions $\beta_{\text{eff}}(v)$ and $\sigma(v)$ are related to the real and imaginary part of the phonon dielectric function $\epsilon_{\text{ph}}(\omega) = \epsilon_1 + i\epsilon_2$ via

$$\beta_{\text{eff}}(v) = \beta_c \epsilon_1, \quad (21)$$

$$\sigma(v) = 1 + v\beta \epsilon_2. \quad (22)$$

Thereby the poles (zeros) of $\epsilon(\omega)$ are given by the eigenfrequencies ω_{TO} (ω_{LO}) of transversal (longitudinal) optical phonons for wavevectors $\vec{k} = 0$. In this way the formalism can be easily extended to an arbitrary number of phonon branches and more complicated lattice dynamical models.

With the help of these relations some special points of the I - V -characteristic $j(v)$ near the subgap structures can be identified:

At the resonance $v = \omega_{\text{TO}}$ of the phononic oscillator the effective quasiparticle conductivity $\sigma(v)$ is strongly enhanced and an analysis of Eq. (17) shows that $\gamma_1(\omega_{\text{TO}}) \approx 0$, which even vanishes exactly for $\rho = 0$. This corresponds to a pure quasiparticle tunneling current across the junction, while the supercurrent and the displacement current are compensating each other.

In contrast to this, the longitudinal optical frequency $v = \omega_{\text{LO}}$ is almost identical with the maximum v_{max} of the I - V -characteristic $j(v)$. The difference $\Delta v := \omega_{\text{LO}} - v_{\text{max}}$ can be estimated as $\Delta v < 2\%$, which is almost independent of the choice of parameters. Therefore the local maximum of the subgap peak located at the frequency ω_{LO} coincides with the zero of the real part ϵ_1 of the phonon dielectric constant. Physically this point is connected with an oscillation of the external electric field E and the polarization p with vanishing displacement current density \dot{D} . Expanding the Besselfunction J_1 in Eq. (18) an analytical formula for the maximal phase

$$\gamma_1(\omega_{\text{LO}}) \approx -4\omega_{\text{LO}}\sigma(\omega_{\text{LO}}) - 8\sqrt{\left(\frac{1}{2}\omega_{\text{LO}}\sigma(\omega_{\text{LO}})\right)^2 + 8} \quad (23)$$

and using Eq. (16) for the maximal current $j(\omega_{\text{LO}})$ can be derived. Thereby it turns out that a small damping parameter ρ , corresponding to a weak coupling of inter-layer ions in neighbouring contacts or equivalently the

small dispersion of the phonons in c-direction, is crucial for the existence of a hysteretic region; no maximum of $j(v)$ can be found for $\rho \geq \rho_{\text{crit}} = \omega_{\text{LO}} - \omega_{\text{TO}}$.

For small voltages $v \ll \Omega$ one has $\beta_{\text{eff}}(v) \approx \beta$ and $\sigma(v) \approx 1$ and the model reduces to the conventional RSJ-model. For this it is well known [4] that there is a voltage jump in the I - V -characteristic at $v_{\text{min}} \approx 4\omega_J/(\pi\omega_c)$.

Moreover, as $\gamma_1 < 0.1$ for relevant parameters, one can expand the equations (16)-(18) up to fourth order in γ_1 and derive

$$\frac{1}{2}\gamma_1^2(v) = \frac{A - \sqrt{A^2 - B}}{B} \quad (24)$$

$$A := 1 + v^4\beta_{\text{eff}}^2 + v^2\sigma^2, \quad B := \frac{78}{48} + 3v^2\sigma^2 + v^4\beta_{\text{eff}}^2.$$

This can be put into Eq. (16) and used to determine $j(v)$ and the differential resistivity dv/dj analytically (cf. figures 1-3).

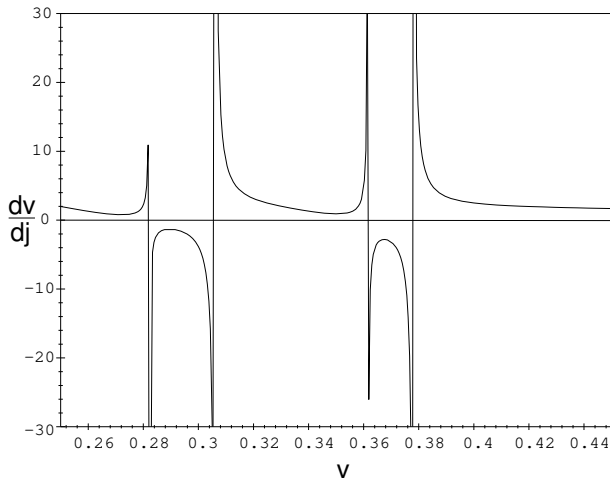


FIG. 1. Analytical solution for the differential resistivity for realistic TBCCO-parameters given in fig. 3.

Note that there exists a region of negative differential resistivity for voltages v slightly larger than ω_{LO} , which cannot be reached in a current-biased experiment with a continuously increasing (decreasing) bias current.

The numerical solution of the differential equations (5) and (6) with a Runge-Kutta-algorithm is in excellent agreement with the analytical results given here, but it is difficult to investigate the region of the I - V -characteristic with negative differential resistivity with this method.

From general results for small capacity β_c [4] it is to be expected that the maximal current j_{max} and the voltage v_{max} of the peak is reduced in the presence of thermal noise. Consequently, the vanishing of the derivative $j'(v)$ near ω_{LO} is rarely observed in experiments or numerical calculations.

In order to reproduce the experimental data in full detail, the shape of the quasiparticle characteristic I_{qp} has to be modified. Instead of the ohmic term $I_{\text{qp}} = \sigma_0\dot{\gamma}$ in Eq. (1) an exponential behaviour

$$I_{\text{qp}}(\dot{\gamma}) \sim \exp\left(\frac{\dot{\gamma}}{v_b}\right) \quad (25)$$

for BSCCO and a semiconductor-like dependence

$$I_{\text{qp}}(\dot{\gamma}) = \frac{2\dot{\gamma}}{1 + \exp\left(\frac{1-\dot{\gamma}}{v_b}\right)} \quad (26)$$

for TBCCO have been used successfully. A detailed theoretical derivation of these phenomenological ansatzes is still missing [5]. The main consequence is a non-linear background $I_{\text{qp}}(v)$ in the I - V -characteristic, while the modifications of the quasiparticle conductivity $\sigma(v)$ are negligible. The shape and the position of the subgap structures are almost independent of the choice of $I_{\text{qp}}(\dot{\gamma})$ and the parameter v_b can be determined very well from parts of the I - V -characteristic away from the subgap structures.

A similar analysis can be carried out for subharmonics $\omega = v/n$ and the corresponding current components j_n , which show a resonance at roughly n times the voltage of the resonance of the first harmonic. Though these higher order peaks are strongly suppressed, they might provide an explanation for small structures seen in experiment at roughly twice the voltage of the main subgap peaks.

For an appropriate choice of parameters these analytical and numerical results are in excellent agreement with the experimental data, as can be seen in figures (2) and (3). All experimental investigations of phonons in TBCCO [6] and BSCCO [7] agree that infrared active c-axis phonons are observed in the frequency range of the subgap structures. Theoretical calculations [8] show that the dispersion in c-direction is small, which corresponds to a small ratio $\rho/(\omega_{\text{LO}} - \omega_{\text{TO}})$ in our model. But considerable discrepancies in the published phonon data do not allow us to use the values given in the literature directly as input parameters. This is also due to the fact that usually only transversal frequencies are determined in optical experiments or model calculations, while the subgap structures should rather be compared with longitudinal branches. Also the precise values of the McCumber parameter β_c and the coupling constant in TBCCO and BSCCO are unknown. Therefore the experimental I - V -characteristics have been fitted with the unconstrained parameters $\beta_c, \Omega_i, \lambda_i, \rho_i$, which turns out to be quite a sensitive method for the determination of these quantities, as an optimal fit seems to be possible only in a very restricted parameter range. As shown above the position of the peaks is given by the zeros of the phonon dielectric constant, which is only dependent on the TO-frequencies Ω_i and the ratios λ_i/β . The absolute values of λ_i and β can be used to tune the relative strength of the peaks, while the values of ρ_i are important for the overall curvature of the structure.

The best fits for TBCCO and BSCCO are given in figures (2) and (3). The prediction for the eigenfrequencies $\nu_{\text{LO}} = \omega_{\text{LO}}(\vec{k} = 0)/(2\pi)$ of the longitudinal optical phonons with lowest frequencies in both materials are in

ordinary units: $\nu_{LO,1}=3.65$ THz and $\nu_{LO,2}=4.70$ THz for TBCCO with a characteristic voltage $V_c = 27.1$ mV and $\nu_{LO,1}=2.96$ THz, $\nu_{LO,2}=3.90$ THz and $\nu_{LO,3}=5.71$ THz for BSCCO with $V_c = 21.8$ mV. These values are compatible with the results of most optical experiments [6,7].

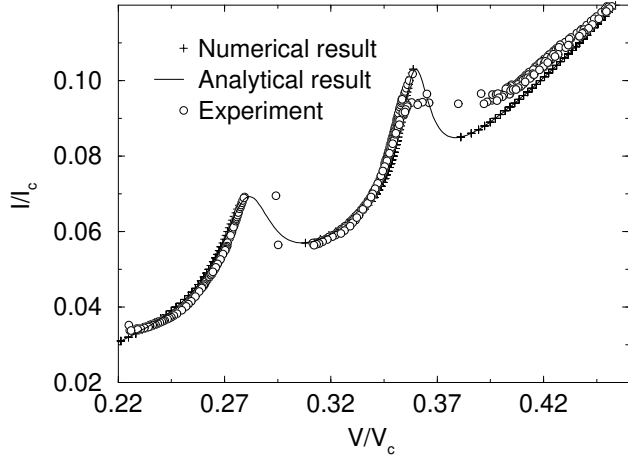


FIG. 2. Experimental, analytical and numerical I - V -characteristic of TBCCO for $\beta_c = 375$, $v_b = 0.29$, $\Omega_1 = 0.25$, $\lambda_1 = 8$, $\rho_1 = 0.03$, $\Omega_2 = 0.34$, $\lambda_2 = 3.5$, $\rho_2 = 0.03$.

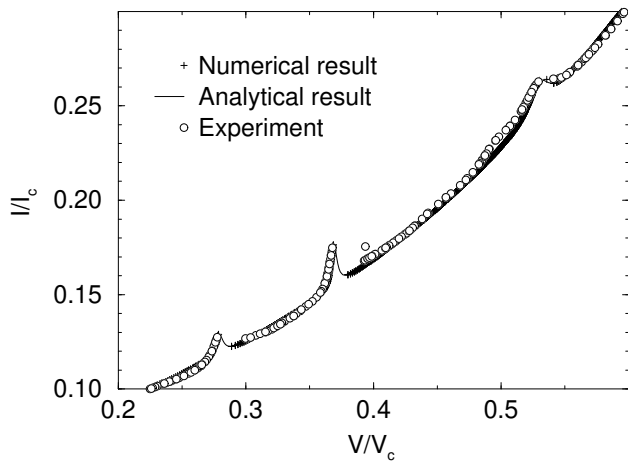


FIG. 3. Experimental, analytical and numerical I - V -characteristic of BSCCO for $\beta_c = 800$, $v_b = 0.337$, $\Omega_1 = 0.267$, $\lambda_1 = 10$, $\rho_1 = 0.008$, $\Omega_2 = 0.345$, $\lambda_2 = 19$, $\rho_2 = 0.0045$, $\Omega_3 = 0.468$, $\lambda_3 = 39$, $\rho_3 = 0.02$.

To summarize, the recently discovered subgap structures in the I - V -characteristic in the intrinsic Josephson-effect in high- T_c -superconductors are explained by a coupling of Josephson oscillations to optical c-axis phonons within a modified RSJ-model. This is – to the knowledge of the authors – the first time that a detailed theoretical explanation of this effect has been given. Apart from perfect reproduction of the experimental data for both BSCCO and TBCCO new insights in the physical interpretation of the peak structures are obtained. Above all, the peak position is identified with the eigenfrequency of the longitudinal optical phonon, which provides a new possibility of a direct measurement of this

quantity, which is normally hard to determine in optical experiments. As a consequence, the position of the subgap structures is expected to depend on pressure and the isotopes contained in the probe. It also turned out that the width of the structure is closely connected with the LO-TO-splitting of the phonon branch.

In principle, similar structures in the current-voltage characteristic can be expected near the zeros of the corresponding dielectric constant, if other kinds of excitations with a dipole moment are coupled to Josephson oscillations between the layers in a similar way. Extensions of this work to a microscopic theory of the Josephson effect within the tunneling Hamiltonian formalism in the presence of phonon bands $\Omega(k_z)$ are currently being investigated. This might help to clarify the reason for the stability of a *local* oscillation despite of the finite coupling of oscillating ions in neighbouring junctions.

Acknowledgment: This work has been supported by a grant of the Bayerische Forschungsstiftung within the research program FORSUPRA and by the Studienstiftung des Deutschen Volkes (C.H.).

-
- [1] R. Kleiner, F. Steinmeyer, G. Kunkel, and P. Müller, Phys. Rev. Lett. 68, 2394 (1992); R. Kleiner, and P. Müller, Phys. Rev. B 49, 1327 (1994).
 - [2] A. Yurgens, D. Winkler, N. Zavaritsky, and T. Claeson, SPIE Proceedings, Conference on Oxide Superconductor Physics and Nano-Engineering II, vol. 2697 (1996).
 - [3] K. Schlenga, G. Hechtfisher, R. Kleiner, W. Walkenhorst, P. Müller, H.L. Johnson, M. Veith, W. Brodkorb, and E. Steinbeiß, Phys. Rev. Lett. 76, 4993 (1996).
 - [4] A. Barone, and G. Paterno. Physics and Application of the Josephson effect. Wiley, New York, 1982.
 - [5] Yu.S. Barach, A.V. Galaktionov, and A.D. Zaikin, Phys. Rev. B 52,1 665 (1995) and references therein.
 - [6] T. Zetterer, M. Franz, J. Schützmann, W. Ose, H.H. Otto, and K.F. Renk, Phys. Rev. B 41, 9499 (1990); V.M. Burlakov, S.V. Shulga, J. Keller, and K.F. Renk, Physica C, 203, 68 (1992) and references therein.
 - [7] R. G. Buckley, M.P. Staines, D.M. Pooke, T. Stoto, and N.E. Flower, Physica C 248, 247 (1995) and references therein.
 - [8] J. Prade, A.D. Kulkarni, F.W. de Wette, U. Schröder, and W. Kress, Phys. Rev. B 39, 2771 (1989); A. D. Kulkarni, F.W. de Wette, J. Prade, U. Schröder, and W. Kress, Phys. Rev. B 43, 7, 5451 (1991).